Atmos. Chem. Phys. Discuss., 7, 10543–10588, 2007
www.atmos-chem-phys-discuss.net/7/10543/2007/

Atmospheric
Chemistry
and Physics
Discussions

# Short- and medium-term atmospheric effects of very large solar proton events

**C. H. Jackman[1], D. R. Marsh[2], F. M. Vitt[2], R. R. Garcia[2], E. L. Fleming[1], G. J. Labow[1], C. E. Randall[3], M. López-Puertas[4], and B. Funke[4]**

[1]NASA/Goddard Space Flight Center, Greenbelt, MD, USA
[2]National Center for Atmospheric Research, Boulder, CO, USA
[3]University of Colorado, Boulder, CO, USA
[4]Instituto de-Astrofisica de Andalucia, CSIC, Granada, Spain

Received: 26 June 2007 – Accepted: 29 June 2007 – Published: 23 July 2007

Correspondence to: C. H. Jackman (charles.h.jackman@nasa.gov)

## Abstract

Solar eruptions sometimes produce protons, which impact the Earth's atmosphere. These solar proton events (SPEs) generally last a few days and produce high energy particles that precipitate into the Earth's atmosphere. The protons cause ionization and dissociation processes that ultimately lead to an enhancement of odd-hydrogen and odd-nitrogen in the polar cap regions (>60° geomagnetic latitude). We have used the Whole Atmosphere Community Climate Model (WACCM3) to study the atmospheric impact of SPEs over the period 1963–2005. The very largest SPEs were found to be the most important and caused atmospheric effects that lasted several months to years after the events. We present the short- and medium-term (days to a few months) atmospheric influence of the four largest SPEs in the past 45 years (August 1972; October 1989; July 2000; and October–November 2003) as computed by WACCM3 and observed by satellite instruments. The polar effects can be summarized as follows: 1) Mesospheric $NO_x$ ($NO+NO_2$) increased by over 50 ppbv and mesospheric ozone decreased by over 30% during these very large SPEs; 2) upper stratospheric and lower mesospheric $NO_x$ increased by over 10 ppbv and was transported during polar night down to the middle stratosphere in a few weeks; 3) mid- to upper stratospheric ozone decreased over 20%; and 4) enhancements of $HNO_3$, HOCl, ClO, $ClONO_2$, and $N_2O_5$ were indirectly caused by the very large SPEs, although the model results suggest impacts at higher altitudes than indicated by the measurements for the October–November 2003 SPE period.

## 1 Introduction

The Earth's atmosphere is occasionally bombarded by a large flux of protons during solar proton events (SPEs). Although relatively infrequent, some of the especially large SPEs have been documented to have a substantial influence on chemical constituents in the polar middle atmosphere, especially $HO_x$, $NO_y$, and ozone (e.g. Weeks et al., 1972; Heath et al., 1977; Reagan et al., 1981; McPeters et al., 1981; Thomas et al., 1983; McPeters and Jackman, 1985; McPeters, 1986; Jackman and McPeters, 1987; Zadorozhny et al., 1992; Jackman et al., 1995, 2001, 2005a; Randall et al., 2001; Seppala et al., 2004, 2006; Lopez-Puertas et al., 2005a, b; von Clarmann et al., 2005; Orsolini et al., 2005; Degenstein et al., 2005; Rohen et al., 2005; Verronen et al., 2006). The influx of solar protons during large events, which are more frequent near solar maximum, can strongly perturb the chemical composition of the polar middle atmosphere via ionization, dissociation, dissociative ionization, and excitation processes.

The important constituent families of $HO_x$ (H, OH, $HO_2$) and $NO_y$ ($N(^4S)$, $N(^2D)$, NO, $NO_2$, $NO_3$, $N_2O_5$, $HNO_3$, $HO_2NO_2$, $ClONO_2$, $BrONO_2$) are produced either directly or through a photochemical sequence as a result of SPEs. The SPE-produced $HO_x$ constituents are important in controlling ozone in the upper stratosphere and mesosphere (pressures less than about 2 hPa). Short-term ozone destruction via the $HO_x$ species proceeds through several catalytic loss cycles such as

$$\begin{array}{l} OH+O_3 \rightarrow HO_2+O_2 \\ \underline{\text{followed by } HO_2+O \rightarrow OH + O_2} \\ \text{Net: } O+O_3 \rightarrow O_2+O_2 \end{array}$$

$$\begin{array}{l} \text{and } H+O_3 \rightarrow OH+O_2 \\ \underline{\text{followed by } OH+O \rightarrow H+O_2} \\ \text{Net: } O+O_3 \rightarrow O_2+O_2. \end{array}$$

The SPE-produced $NO_x$ constituents lead to short- and longer-term catalytic ozone destruction in the lower mesosphere and stratosphere (pressures greater than about 0.5 hPa) via the well-known $NO_x$-ozone loss cycle

$$\begin{array}{l} NO + O_3 \rightarrow NO_2+O_2 \\ \underline{\text{followed by } NO_2+O \rightarrow NO+O_2} \\ \text{Net: } O+O_3 \quad \rightarrow O_2+O_2. \end{array}$$

There have been a number of modeling studies focused on understanding and predicting the atmospheric influence of SPEs (e.g. Warneck, 1972; Swider and Keneshea, 1973; Crutzen et al., 1975; Swider et al., 1978; Banks, 1979; Fabian et al., 1979; Jackman et al., 1980, 1990, 1993, 1995, 2000, 2007; Solomon and Crutzen, 1981; Rusch et al., 1981; Solomon et al., 1981, 1983; Reagan et al., 1981; Jackman and McPeters, 1985; Roble et al., 1987; Reid et al., 1991; Vitt and Jackman, 1996; Vitt et al., 2000; Krivolutsky et al., 2001, 2003, 2005, 2006; Verronen et al., 2002, 2005, 2006; Semeniuk et al., 2005). Most of these studies were carried out with lower dimensional models (0-D, 1-D, 2-D); however, a few used three-dimensional (3-D) models (e.g. Jackman et al., 1993, 1995, 2007; Semeniuk et al., 2005; Krivolutsky et al., 2006) to investigate the more detailed global effects of SPEs.

In this study we have used version 3 of the Whole Atmosphere Community Climate Model (WACCM3), which is a general circulation model with complete interactive photochemistry with a domain that extends from the ground to the lower thermosphere. The recent development of WACCM3 allows study of the detailed time-dependent 3-D atmospheric response to a variety of perturbations. The purpose of this work is to use WACCM3 to investigate the global effects of SPEs over solar cycles 20–23 (years 1963–2005). The short- and medium-term (days to months) atmospheric influence will be shown with particular attention to the SPE-induced changes in stratospheric and mesospheric (middle atmospheric) composition. We have observations from several satellite instruments documenting SPE effects during the most recent solar maximum period (solar cycle 23, years 2000–2005) to help verify WACCM3 predictions. We also have a few satellite instrument measurements of atmospheric impacts during the very large SPEs of August 1972 and October 1989 with which to compare.

This paper is divided into seven primary sections, including the Introduction. The solar proton flux and ionization rate computation are discussed in Sect. 2 and SPE-induced production of $HO_x$ and $NO_y$ are discussed in Sect. 3. A description of the satellite instrument measurements and WACCM3 is given in Sect. 4. WACCM3 model results for short-term (days) constituent changes, with comparisons to measurements for some very large SPEs of the past 45 years, are shown in Sect. 5 while medium-term (months) constituent changes caused by SPEs are discussed in Sect. 6. The conclusions are presented in Sect. 7.

## 2 Proton measurement/ionization rates

Solar proton fluxes have been measured by a number of satellites in interplanetary space or in orbit around the Earth. The National Aeronautics and Space Administration (NASA) Interplanetary Monitoring Platform (IMP) series of satellites provided measurements of proton fluxes from 1963–1993 (Jackman et al., 1990; Vitt and Jackman, 1996). The National Oceanic and Atmospheric Administration (NOAA) Geostationary Operational Environmental Satellites (GOES) were used for proton fluxes from 1994–2005 (Jackman et al., 2005b).

Proton flux data from IMP 1–7 were used for the years 1963–1973. These data were taken from T. Armstrong and colleagues (University of Kansas, private communication, 1986; see Armstrong et al. (1983) for a discussion of the IMP 1–7 satellite measurements). A power law was used to fit these flux data as a function of energy, which were assumed to be valid over the range 5–100 MeV (Jackman et al., 1990) and then degraded in energy using the scheme first discussed in Jackman et al. (1980). The scheme includes the deposition of energy by all the protons and associated secondary electrons. The energy required to create one ion pair was assumed to be 35 eV (Porter et al., 1976).

IMP 8 was used for the proton flux data for the years 1974–1993. Vitt and Jackman (1996) take advantage of the measurements of alpha particles by IMP 8 as well and use proton fluxes from 0.38–289 MeV and alpha fluxes from 0.82–37.4 MeV in energy deposition computations. The energy deposition methodology is similar to that discussed in Jackman et al. (1980). Alpha particles were found to add about 10% to the total ion pair production during SPEs.

Four GOES satellites are used for the proton fluxes in years 1994–2005: 1) GOES-7 for the period 1 January 1994 through 28 February 1995; 2) GOES-8 for the period 1 March 1995 through 8 April 2003, and 10 May 2003 to 18 June 2003; 3) GOES-11 for the period 19 June 2003 to 31 December 2005; and 4) GOES-10 to fill in the gap of missing proton flux data from 9 April through 9 May 2003. The GOES satellite proton fluxes are fit with exponential spectral forms in three energy intervals: 1–10 MeV, 10–50 MeV, and 50–300 MeV. The energy deposition methodology again is that discussed in Jackman et al. (1980).

The daily average ion pair production rates for years 1963–2005 were computed from the energy deposition assuming 35 eV/ion-pair. An example of the daily average ionization rate ($cm^{-3} s^{-1}$) is given in Fig. 1 for a thirteen day period in October–November 2003, a very intense period of SPEs. The 28–31 October 2003 SPE period was the fourth largest of the past 45 years (see Table 1). Very large daily average ionization rates of >5000 $cm^{-3} s^{-1}$ extending from 0.01 to 1 hPa are computed for 29 October 2003. Large ionization rates >1000 $cm^{-3} s^{-1}$ extending from the upper stratosphere through the mesosphere are computed for 28–30 October 2003.

These ionization rate data are provided as functions of pressure between 888 hPa (~1 km) and $8\times10^{-5}$ hPa (~115 km) at the SOLARIS (Solar Influence for SPARC) website (http://strat-www.met.fu-berlin.de/~matthes/sparc/inputdata.html) and can be used in model simulations.

## 3 Odd hydrogen ($HO_x$) and odd nitrogen ($NO_y$) production

### 3.1 Odd hydrogen ($HO_x$) production

Protons and their associated secondary electrons also produce odd hydrogen ($HO_x$). The production of $HO_x$ takes place after the initial formation of ion-pairs and is the end result of complex ion chemistry (Swider and Keneshea, 1973; Frederick, 1976; Solomon et al., 1981). Generally, each ion pair results in the production of approximately two $HO_x$ species in the upper stratosphere and lower mesosphere. In the middle and upper mesosphere, an ion pair is calculated to produce less than two $HO_x$ species. The $HO_x$ production from SPEs is included in WACCM3 using a lookup table from Jackman et al. (2005a, Table 1), which is based on the work of Solomon et al. (1981). The $HO_x$ constituents are quite reactive with each other and have a relatively short lifetime (∼ hours) throughout most of the mesosphere (Brasseur and Solomon, 1984, see Fig. 5.28) and thus are important only during and shortly after solar events.

### 3.2 Odd nitrogen ($NO_y$) production

Odd nitrogen is produced when the energetic charged particles (protons and associated secondary electrons) collide with and dissociate $N_2$. We assume that ∼1.25 N atoms are produced per ion pair and divide the proton impact of N atom production between ground state (∼45% or ∼0.55 per ion pair) and excited state (∼55% or ∼0.7 per ion pair) nitrogen atoms (Porter et al., 1976). Following the discussion in Jackman et al. (2005a), we assume production of 0.55 ground state $N(^4S)$ per ion pair and 0.7 $N(^2D)$ atoms per ion pair for our model simulations.

SPEs can also lead to a reduction in odd nitrogen via production of $N(^4S)$, when the $NO_y$ loss reaction, $N(^4S)+NO \rightarrow N_2+O$, is increased. This $NO_y$ loss mechanism is important during especially large SPEs, when a huge amount of $NO_y$ is produced in a short period of time (Rusch et al., 1981). In spite of the associated enhanced loss of $NO_y$ during these disturbed periods, SPEs will result in an increase in $NO_y$ constituents on the whole. Figure 2 shows a time series of our computed annually averaged global $NO_y$ production from SPEs in the middle atmosphere. The $NO_y$ production roughly follows the solar cycle with maximum (minimum) production near sunspot maximum (minimum).

Although the solar UV-induced oxidation of nitrous oxide ($N_2O+O(^1D) \rightarrow NO+NO$) provides the largest source of $NO_y$ in the middle atmosphere (52–58 gigamoles per year; Vitt and Jackman 1996), the SPE source of $NO_y$ can be significant during certain years. This is especially true at polar latitudes where the transport from lower latitudes and the larger solar zenith angles result in a somewhat smaller local source of $NO_y$ due to $N_2O$ oxidation. Table 1 shows the magnitude of the fifteen largest individual SPEs, in terms of the computed middle atmospheric $NO_y$ production, during the past 45 years. Note that eight of these event periods occurred during the current solar cycle.

The $NO_y$ family can have a lifetime of months to years, if it is transported to the middle and lower stratosphere (e.g. Randall et al., 2001; Jackman et al., 2005a). Therefore, the effects of the SPE-produced $NO_y$ can last for several months, especially when large solar events occur in late fall or winter.

## 4 Model and measurement information

### 4.1 Description of the Whole Atmosphere Community Climate Model (WACCM3)

WACCM3 is a relatively new model with a domain from the surface to 140 km and 66 vertical levels. Vertical resolution is $\leq$1.5 km between the surface and about 25 km. Above that altitude, vertical resolution increases slowly to 2 km at the stratopause and 3.5 km in the mesosphere; beyond the mesopause, the vertical resolution is one half the local scale height. The latitude and longitude grids have spacing of 4° and 5°, respectively. The model has fully interactive dynamics, radiation, and chemistry. WACCM3 incorporates modules from the Community Atmospheric Model (CAM3), the Thermosphere-Ionosphere-Mesosphere-Electrodynamics General Circulation Model (TIME-GCM), and the Model for Ozone And Related chemical Tracers (MOZART-3) to simulate the dynamics and chemistry of the Earth's atmosphere. This model has been developed over the past seven years and has become a useful tool for investigating the coupling among the various atmospheric regions from the troposphere through the middle atmosphere to the lower thermosphere (Sassi et al., 2002, 2004; Forkman et al., 2003; Richter and Garcia, 2006; Garcia et al., 2007).

### 4.2 WACCM3 simulations

WACCM3 was forced with observed time-dependent sea surface temperatures (SSTs), observed solar spectral irradiance and geomagnetic activity changes, and observed concentrations of greenhouse gases and halogen species over the simulation periods (see Garcia et al., 2007). We have completed a number of WACCM3 simulations, some with the daily ionization rates from SPEs and some without. The ionization rates, when included, were applied uniformly over both polar cap regions (60–90° N and 60–90° S geomagnetic latitude) as solar protons are guided by the Earth's magnetic field lines to these areas (McPeters et al., 1981; Jackman et al., 2001, 2005a). The effects are not expected to be symmetric between the hemispheres because of the differing offsets of geomagnetic and geographic poles. A list of the WACCM3 simulations and their designation in this study is given in Table 2.

Since the year 1989 was very active in terms of SPEs (see Table 1), simulations with SPEs (see 2 a,b,c,d) and without SPEs (see 2 w,x,y,z) were performed to study the 15 month period, 1 January 1989–31 March 1990. The very large July 2000 SPE was studied in further detail over the period 2 July–30 September 2000 using simulations with SPEs (see 3 a,b,c,d) and without SPEs (see 3 w,x,y,z). The very large late October/early November 2003 SPEs were studied in further detail over the period 25 October–14 November 2003 using a simulation with SPEs (see 4 a) and without SPEs (see 4 w). Simulations 1(a,b,c,d), 2(a,b,c,d), and 2(w,x,y,z) have model output every five days. Simulations 3(a,b,c,d), 3(w,x,y,z), 4(a), and 4(w) have model output every day. For short periods (~two weeks), different realizations produce similar results; thus it is appropriate to use only a single realization for simulation 4.

### 4.3 Satellite instrument measurements

Several satellite instruments have recorded atmospheric constituent change caused by SPEs. We will compare WACCM3 results with:

1) Nimbus 4 Backscatter Ultraviolet (BUV) ozone measurements (August 1972

SPEs);

2) Stratospheric Aerosol and Gas Experiment (SAGE) II ozone and $NO_2$ and NOAA 11 Solar Backscatter Ultraviolet 2 (SBUV/2) ozone measurements (October 1989 SPEs);

3) NOAA 14 SBUV/2 ozone and Upper Atmosphere Research Satellite (UARS) Halogen Occultation Experiment (HALOE) $NO_x$ (July 2000 SPE);

and 4) UARS HALOE $NO_x$ and Envisat Michelson Interferometer for Passive Atmospheric Sounding (MIPAS) ozone, $NO_x$, $HNO_3$, $N_2O_5$, and HOCl (October/November 2003 SPEs).

## 5 SPE-induced short-term (days) changes in composition

The very large SPEs (see Table 1) caused the most profound changes in atmospheric composition. Satellite instrument observations exist for several constituents during SPEs that occurred in solar cycle 23. The October 2003, July 2000, August 1972, and October 1989 SPEs – the fourth, third, second, and first largest SPE periods in the past 45 years, respectively – were ideal candidates for comparing WACCM3 results to measurements. Previous studies of these four SPE periods have documented significant changes associated with the events (e.g. Heath et al., 1977; Reagan et al., 1981; McPeters et al., 1981; Jackman and McPeters, 1987, 2004; Jackman et al., 1990, 1993, 1995, 2001, 2005a; Zadorozhny et al., 1992; Randall et al., 2001; Seppala et al., 2004; Degenstein et al., 2005; Lopez-Puertas et al., 2005a, b; Orsolini et al., 2005; von Clarmann et al., 2005; Rohen et al., 2005). We compare the WACCM3 results with some of these satellite measurements in Sects. 5.2 through 5.4.

Several large solar eruptions occurred in October/November 2003, the so-called “Halloween Storms”. The most intense SPE period accompanying these solar eruptions was during 28–31 October 2003, the fourth largest SPE period in the past 45 years. The atmospheric effects from these SPEs are probably the best documented for any solar events. At least five satellite instruments measured the atmospheric effects of these SPEs, including UARS HALOE, NOAA-16 SBUV/2, and Envisat's MIPAS, SCIAMACHY, and GOMOS (Seppala et al., 2004; Jackman et al., 2005a; Lopez-Puertas et al., 2005a, b; von Clarmann et al., 2005; Orsolini et al., 2005; Degenstein et al., 2005; Rohen et al., 2005). The middle atmospheric effects from the SPEs were largest during and several days after these events.

To be clear: We focus only on the impact of the solar protons associated with the solar eruptions in October–November 2003. It is likely that huge increases in lower thermospheric $NO_x$ were created by lower-energy electron precipitation, which occurred in conjunction with these SPEs. The very large enhancements in mesospheric and upper stratospheric $NO_x$ observed by UARS HALOE, the Canadian Space Agency (CSA) Atmospheric Chemistry Experiment (ACE), and MIPAS in the Northern Hemisphere in February–April 2004 were possibly caused by the downward transport of this thermospheric $NO_x$ to lower atmospheric levels (Natarajan et al., 2004; Rinsland et al., 2005, and Randall et al., 2005).

### 5.1 $HO_x$ (H, OH, $HO_2$) constituents

The "Halloween Storms" of 2003 caused SPEs, which produced $HO_x$ constituents. The $HO_x$ changes simulated by WACCM3 are presented in Fig. 3 for the southern (70–90° S; left) and northern (70–90° N; right) polar regions from simulation 4(a). Huge $HO_x$ increases are predicted during the most intense periods of the SPEs reaching over 100% and 700% near 0.1 hPa in the southern and northern polar regions, respectively. Since the $HO_x$ species have a relatively short lifetime (hours), these very short-term effects disappear almost entirely by the end of 6 November. $HO_x$ changes after this date are due to the normal seasonal behavior in those regions as sunlight increases (decreases) in the southern (northern) polar regions at this time of year, leading to increases (decreases) in $HO_x$ as the sources of $HO_x$ [$H_2O+O(^1D)\rightarrow 2OH$ and $H_2O+h\nu\rightarrow H+OH$] are affected. The enhanced $HO_x$ constituents produced by the SPEs led to short-term ozone destruction, especially in the mesosphere and upper stratosphere.

### 5.2 $NO_x$ (N, NO, $NO_2$) constituents

The $NO_x$ species have considerably longer lifetimes than the $HO_x$ species and are produced in great abundance during very large SPEs. For example, we have evidence of huge enhancements of $NO_x$ as a result of the “Halloween Storms” of 2003. The Envisat MIPAS instrument provided simultaneous observations of $NO_x$ in both polar regions. Atomic nitrogen (N) is quite small in the mesosphere and stratosphere; thus, the MIPAS measurements of NO and $NO_2$ essentially provide a measure of the polar $NO_x$ enhancements during the “Halloween Storms” of 2003. We show the MIPAS Northern Hemisphere polar $NO_x$ on three days (27, 29, and 30 October) in Fig. 4 (top) at the 2250 K (50–55 km) surface. The polar vortex edge has been calculated using the Nash criterion (Nash et al., 1996) but modified so that a dynamical tracer ($CH_4$ below 1500 K and CO above) has been used, instead of the mean zonal winds. This vortex boundary is represented with a red curve and the geomagnetic pole is marked with a red plus sign. Some individual $NO_x$ values reached 180 ppbv, about a factor of ten larger than normal under unperturbed conditions. Generally, the largest average $NO_x$ values were close to 100 ppbv.

We present WACCM3 results for the same three days in Fig. 4 (bottom) from simulation 4(a). The model shows similar qualitative and quantitative behavior with polar $NO_x$ levels reaching over 90 ppbv. There are differences in the shape of the SPE-perturbed region, which are probably due to differences between the transport in WACCM3 and the Earth’s atmosphere at this level. WACCM3 is a free-running climate model, so the computations cannot be expected to reproduce in detail the conditions prevailing in the atmosphere at any particular time.

$NO_x$ levels were also measured during this period by UARS HALOE. We show the excess $NO_x$ beyond baseline amounts before the SPE period in our Fig. 5 (left) (taken from Fig. 7 of Jackman et al., 2005a). This plot was constructed with HALOE profiles taken at high southern latitudes in the SPE-disturbed period 30 October–7 November 2003 compared to those taken at high southern latitudes before the SPE (12–15

October 2003).

We present WACCM3 results from simulation 4(a) for $NO_x$ during this same period in Fig. 5 (right). The values in the plot show the excess $NO_x$ beyond the 25 October 2003 levels (quiet period). Both the observations and the model indicate a very similar temporal structure. Huge $NO_x$ increases of greater than 100 ppbv were produced in the middle to upper mesosphere (0.03 to 0.006 hPa) for 30–31 October . The lower mesosphere showed $NO_x$ increases of greater than 20 ppbv throughout the period, compared with unperturbed values of less than 1 ppbv (Jackman et al., 2005a). There are some modest differences between the WACCM3 predictions and the HALOE measurements. There appears to be a larger amount of modeled $NO_x$ on 7 November between about 0.7 and 3 hPa than shown in the measurements. However, given the huge $NO_x$ changes from this perturbation, WACCM3 and HALOE are in reasonable agreement.

### 5.3 Ozone

Ozone was also impacted by these SPEs. The SPE-produced $HO_x$ and $NO_x$ constituents led to short- and longer-term catalytic ozone destruction in the lower mesosphere and stratosphere (pressures greater than about 0.5 hPa). The temporal evolution of changes in ozone abundance measured by MIPAS during and after the October–November 2003 SPEs is given in Fig. 6 (top). These values are presented for the Southern Hemisphere (SH) (70–90° S) and Northern Hemisphere (NH) (70–90° N) polar caps. The measurements are compared to WACCM3 predictions from simulation 4(a) in the same regions in Fig. 6 (bottom). Due to the short lifetime of $HO_x$ constituents (see Fig. 3), their ozone influence lasts only during and for a few hours after the SPEs. This explains the huge measured and modeled ozone depletion on 29–30 October and, to a lesser extent, on 3–4 November. Note that Fig. 1 shows ion pair production, which is essentially a proxy for the $NO_x$ and $HO_x$ production.

SPE impacts in the NH are larger than the SH in both models and simulations. NH ozone depletion exceeds 50% during the SPEs in late October. Polar NH upper stratospheric ozone depletion greater than 30% continues through 14 November, the end of the plotting period. The polar SH shows ozone reduction greater than 30% during the SPEs in late October with lower mesospheric ozone depletion from 5–10% continuing through 14 November.

The measured and modeled ozone depletions do show some differences. The NH modeled ozone indicates a larger recovery (ozone enhancement) above ~57 km after 7 November, than indicated in the measurements. This apparent NH ozone recovery is due to seasonal changes, wherein ozone is enhanced via transport from above. The SH modeled ozone below ~45 km indicates a larger ozone depletion after 2 November, than indicated in the measurements. The reason(s) behind these NH and SH model-measurement differences are still unclear, but is probably caused in part by the fact that transport in WACCM is not meant to simulate any specific year.

Other measurements of short-term ozone loss caused by solar protons are available for other SPEs. For example, a very large SPE commenced on 14 July 2000, the so-called "Bastille Day" solar storm, which was the third largest SPE period in the past 45 years. This SPE took place over the 14–16 July period. Jackman et al. (2001) showed Northern Hemisphere polar ozone changes (in ppmv) from the NOAA 14 SBUV/2 instrument at 0.5 hPa due to the July 2000 SPE between 13 July (before SPE) and 14–15 July (during SPE), 2000. We provide a similar plot in Fig. 7, which shows the percentage change for ozone from 13 July to 14–15 July for NOAA 14 SBUV/2 and from 13 July to 15 July at 0:00 GMT from WACCM3 simulation 3(a). Figure 7 (left) is constructed from 24 h of NOAA 14 SBUV/2 orbital data during the maximum intensity of the event and Fig. 7 (right) is a difference of model "snapshots."

The polar cap edge (60° geomagnetic latitude), wherein the protons are predicted to interact with the atmosphere, is indicated by the white circle. Large ozone decreases of 30–40% are seen at this pressure level in both the SBUV/2 observations and WACCM3 calculations, which are primarily caused by the SPE. These ozone decreases are driven by catalytic destruction from the $HO_x$ increases of ~100% and are mostly confined to the polar cap areas (e.g. Jackman et al., 2001). Overall there is good agreement between WACCM3 and SBUV/2.

### 5.4 Other constituents

Several other constituents appear to have been influenced as a result of the SPEs during the "Halloween Storms" of 2003, including $HNO_3$, HOCl, ClO, $ClONO_2$, and $N_2O_5$ (Orsolini et al., 2005; von Clarmann et al., 2005; Lopez-Puertas et al., 2005b). We show WACCM3 comparisons with three of these constituents, $HNO_3$, $N_2O_5$. and HOCl. Figure 8 (top) shows the temporal change in Envisat MIPAS $HNO_3$ during the nighttime in the polar Northern Hemisphere (70–90° N). This figure was taken from Fig. 2a of Lopez-Puertas et al. (2005b), who argued that the increases in $HNO_3$ from 30–45 km were probably caused primarily by the gas-phase reaction, $NO_2+OH+M \rightarrow HNO_3+M$. Both OH and $NO_2$ enhancements were simulated when WACCM3 was run *with* SPEs and this reaction leads to increases in $HNO_3$. However, the model results from simulation 4(a) (see Fig. 8 (middle)) suggest that $HNO_3$ increases were largest above 45 km and below 30 km in the period plotted. Figure 8 (bottom) shows WACCM3 results from a simulation *without* SPEs, simulation 4(w), which indicates that there are seasonal changes below 35 km forcing an enhancement in $HNO_3$ at this time of year. The length of night is gradually increasing in late October and November, which leads to an increase in the reservoir species (including $HNO_3$). It is difficult to understand the significant observed changes in the 30–45 km altitude range, given the ionization rates of Fig. 1, without involving some other pathway for $HNO_3$ production such as ion chemistry. Lopez-Puertas et al. (2005b) discussed the following ion chemistry scheme for $HNO_3$ production:

$$O_2^+ H_2O+H_2O \rightarrow H_3O^+ \cdot OH+O_2$$

$$H_3O^+ \cdot OH+H_2O \rightarrow H^+ \cdot (H_2O)_2+OH$$

$$H^+ \cdot (H_2O)_2+NO_3^- \rightarrow HNO_3+H_2O + H_2O$$

$$\text{Net}: H_2O+NO_3 \rightarrow HNO_3+OH$$

This pathway for $HNO_3$ production, first proposed by Solomon et al. (1981), requires the production of $NO_3^-$ and functions under dark conditions. Such a scheme is presently not included in WACCM3 computations.

Envisat MIPAS measurements and WACCM3 computations of $N_2O_5$ are presented for the polar Northern Hemisphere (70–90° N) in Fig. 9. The temporal change in Envisat MIPAS $N_2O_5$ during the nighttime in the polar Northern Hemisphere (70–90° N) is taken from Fig. 5 of Lopez-Puertas et al. (2005b) and shown in Fig. 9 (top). The $N_2O_5$ modeled [simulation 4(a)] enhancements peaked between 30 and 50 km near the last day plotted (14 November), similar to the MIPAS observations. WACCM3 predicted $N_2O_5$ increases of 5–6 ppbv (primarily driven by the SPEs) were, however, significantly larger than the MIPAS measured increases of about 1 ppbv. WACCM3 predicted seasonal changes in $N_2O_5$ are shown in Fig. 9 (bottom) from a computation *without* SPEs [simulation 4(w)]. This plot indicates the importance of the seasonal changes in forcing the $N_2O_5$ enhancement of 0.6 ppbv between 25 and 35 km from 26–31 October 2003. The seasonal changes contribute only modestly to the $N_2O_5$ increases in the mid- to upper stratosphere (30–50 km) in November 2003, so the cause of the discrepancy between the model and measurements at these altitudes is not understood.

Envisat MIPAS measurements and WACCM3 computations of HOCl simulation 4(a) are presented for the polar Northern Hemisphere (70–90° N) in the top and bottom of Fig. 10, respectively. Both model and measurement show very significant HOCl enhancements in the altitude range 35–55 km. The mechanism for increasing HOCl as a result of the SPEs involves enhancing the $HO_x$ constituents, which then speed up the following gas-phase three reaction sequence:

$$OH+HCl \rightarrow H_2O+Cl$$

$$Cl+O_3 \rightarrow ClO+O_2$$

$$ClO+HO_2 \rightarrow HOCl+O_2.$$

Generally, the measurements and model predictions are in agreement, although there is a slight disagreement in the altitude range of the effect. The measurements indicate HOCl increases all the way down to 30 km, whereas WACCM3 calculates HOCl increases from 35 km up to 60 km and above. Both measurements and model show a HOCl peak on 29 October; however, the WACCM3 peak is about 0.1–0.15 ppbv larger. WACCM3 results also show a secondary HOCl peak on 4 November due to a smaller SPE in this period (Fig. 1). We also investigated model predictions in the WACCM3 computation *without* SPEs [simulation 4(w)] and found very small changes over this period, implying that most of the measured and modeled HOCl changes were due to the SPEs.

Our simulations also provided information on ClO and $ClONO_2$ changes during and shortly after the SPEs during the “Halloween Storms” of 2003, which are not shown in this study. WACCM3 ClO enhancements peaked near 0.3 ppbv on 29 October similar to the MIPAS observations (von Clarmann et al., 2005). However, the model enhancements were largest above 50 km and the MIPAS increases were largest between about 35 and 45 km. The predicted $ClONO_2$ increases caused by the SPEs maximized over 0.3 ppbv about a week after the largest proton fluxes on 29–30 October similar to the MIPAS observations (von Clarmann et al., 2005; Lopez-Puertas et al., 2005). The $ClONO_2$ modeled enhancements were largest between 40 and 50 km and the MIPAS $ClONO_2$ measured increases were largest below 40 km, peaking between 30 and 33 km.

Overall it seems the modeled enhancements in $HNO_3$, HOCl, ClO, $ClONO_2$, and $N_2O_5$ tend to be higher in altitude than indicated in the measurements. These model/measurement differences seem to be caused, at least partially, by an overly strong smoothing constraint applied to the retrieval of MIPAS species abundances. The Tikhonov smoothing operator used in the MIPAS retrieval was originally optimized for unperturbed conditions. New retrievals performed with a more relaxed regularization allow a better vertical resolution. For a few days in this period these new retrievals show generally that the altitude of the peak of the enhancement is located at higher altitudes, as WACCM3 predicts. In particular, the MIPAS re-processed $HNO_3$, also shows two enhanced layers, the lower one at ~25 km, explained by the model by the seasonal change, and the SPE-induced enhanced layer at around 45–50 km. The re-processed $ClONO_2$ also shows an enhancement at higher altitudes, around 35–45 km, but still some ∼5 km lower than in the model. Hence the re-processed data for $HNO_3$ and $ClONO_2$ shows a much better agreement but still about 5 km lower in the measurements. We should have in mind that this altitude shift is similar to the vertical resolution of MIPAS for those species in this region, of about 4–5 km.

The re-processed $N_2O_5$ abundance does not exhibit, however, any significant change. Hence, the model clearly overestimates the measurements. Since the production of $N_2O_5$ is very sensitive to the temperature, differences between the predicted/real temperatures, and/or differences in the dynamics (downward transport of earlier-produced $NO_2$) might explain these differences.

## 6 SPE-induced medium-term (months) changes in composition

### 6.1 July 2000 Solar Proton Event

The July 2000 SPE produced huge amounts of $NO_x$, which was observed by HALOE and simulated in a 2-D model (Jackman et al., 2001). We computed an ensemble average of the two groups of simulations 3(a,b,c,d) and 3(w,x,y,z) and differenced the two to derive the results shown in Fig. 11. Note the near anti-correlation of $NO_x$ (Fig. 11, left) and ozone (Fig. 11, right) over most of this period. The $HO_x$ constituents (not shown) produced during the SPE on days 196–198 (14–16 July) are responsible for the short-lived large ozone decreases (>40%). The SPE-caused enhanced $NO_x$ then drives the ozone depletion after this period. By about day 255 (11 September), a $NO_x$ increase of >5 ppbv appears to cause an ozone loss of >10%. The rate of descent of the $NO_x$ and ozone perturbation is about 140 m/day (∼0.16 cm/s) over this period.

Is there any evidence of SPE-caused $NO_x$ enhancements lasting at least six weeks after the event period, as simulated by WACCM3? Yes: Randall et al. (2001) showed evidence from HALOE observations of large $NO_x$ ($NO+NO_2$) enhancements two months after this July 2000 SPE in the Southern Hemisphere. The $NO_x$ increases in September 2000 in the polar vortex were almost certainly caused by the July 2000 SPE (see Fig. 12, left). Ten years of HALOE observations are presented in Fig. 12 (left). Although there is evidence of interannual variability, the year 2000 shows enhancements of $NO_x$ by about a factor of 2–3 beyond the normal range near 1000 K (~33 km).

We have sampled the WACCM3 output of simulation 1(a) in a similar manner and present the results in Fig. 12 (right side). The WACCM3 results indicate somewhat larger interannual variability above about 32 km, and less variability below this altitude. However, year 2000 shows a clear enhancement beyond the normal range that is analogous to the HALOE measurements. The sharper peak in WACCM3 is likely related to the coarser altitude grid in the model. There are differences in the interannual variability in WACCM3 compared with HALOE near the top level shown (1500 K, ~40 km) in Fig. 12. It is unclear what the differences in variability mean, although a strong possibility is different dynamics in the model and actual atmosphere. For instance, the local maxima near 700–800 K in the HALOE data likely result from downward transport of $NO_x$ produced earlier in the winter at higher altitudes by energetic particle precipitation (see Randall et al., 2007); WACCM3 might not be simulating this transport adequately. Recall that since the version of WACCM3 used here is not forced by analyzed winds, we do not expect the model dynamics to match the atmospheric dynamics in detail for any specific year.

### 6.2 August 1972 Solar Proton Events

The second largest SPE period in the past 45 years occurred 2–10 August 1972 (days 215–223). Although this SPE period occurred about 35 years ago, there were recorded measurements of its ozone impact (e.g. Heath et al., 1977; Reagan et al., 1981; McPeters et al., 1981; Jackman and McPeters, 1987; Jackman et al., 1990). We compare our WACCM3 predicted ozone changes to measured ozone changes from the backscattered ultraviolet (BUV) instrument on the Nimbus 4 satellite between about

32 and 53 km for 60 days in Fig. 13. The BUV changes (Fig. 13a) were derived by comparing 1972 to 1970 ozone data (Jackman et al., 1990) in latitude band 70–80° N. The WACCM3 computed ozone changes (Fig. 13b) were derived by averaging the ensemble of simulations 1(a,b,c,d) and comparing 1972 to 1970 for the same latitude band.

There is reasonable agreement between the model and measurement with both showing significant ozone depletion (>10%) in the upper stratosphere (~40–50 km) over most of the 60-day time period in the 70–80° N latitude band. Both model and measurement show modest ozone depletion (5–10%) in the altitude region 40–45 km over most of the period in the 50–60° N latitude band (not shown). There are also some differences with the measurements indicating a larger ozone depletion in the 33–40 km region for both latitude bands than simulated by the model. As explained in Jackman et al. (2000), only proton fluxes with energies less than 100 MeV were included for these SPEs. The August 1972 events probably did have protons with energies greater than 100 MeV, which affect altitudes below 35 km. These high-energy protons, however, could not be reliably included into our computations.

### 6.3 October 1989 Solar Proton Events

The largest SPE period in the past 45 years occurred 19–27 October (Days 292–300), 1989. The $NO_y$ produced during this period was nearly a factor of two larger than the second largest SPE period (see Table 1). Both rocket measurements (NO; Zadorozhny et al., 1992) and satellite measurements (ozone and $NO_2$; Jackman et al., 1993, 1995) showed atmospheric changes as a result of these extremely intense SPEs.

We computed an ensemble average of the two groups of simulatios 2(a,b,c,d) and 2(w,x,y,z) and differenced the two to derive the percentage change shown for $NO_2$ (Fig. 14, top) and ozone (Fig. 14, bottom) at 70° N. Very large upper stratospheric enhancements of $NO_2$ greater than 100% from late October to early December drive ozone decreases greater than 20%. The substantial ozone depletion (>10%) between 2 and 4 hPa before the 19–27 October SPE period was mainly caused by prior large

SPE periods in 13–26 August 1989 and 29 September–3 October 1989 (see Table 1), which produced sufficient $NO_x$ to cause a longer-lived ozone loss.

We computed the ozone change in the latitude band 60–80° from the WACCM3 simulations 2(a,b,c,d) at 4 hPa (December 1989 contrasted with the December 1990 and December 1991 average) to be: 1) –6% for the SH; and 2) –18% for the NH. These model results can be compared to the NOAA 11 SBUV/2 measurements taken from Jackman et al. (1995), see Table 1 of: 1) –1% for the SH; and 2) –12% for the NH. Although there are quantitative differences between WACCM3 and SBUV/2 measurements, the prediction of a substantially larger ozone depletion in the NH than the SH in December 1989 is similar to the measurements. These WACCM3 results complement the three-dimensional chemistry-transport-model results given in Jackman et al. (1995).

SAGE II ozone and $NO_2$ measurements over five months after this extreme proton flux period have been reported before in a comparison with 3D model predictions (Jackman et al., 1995). SAGE II observations and WACCM3 simulation results are presented for $NO_2$ (Fig. 15, top) and ozone (Fig. 15, bottom) for 31 March 1990. The SAGE II observations were derived by computing the percentage difference on 31 March 1990 compared with 31 March 1987 and are represented by the solid line with asterisks. WACCM3 (case 1) results, represented by the dotted line, were derived using the ensemble mean of simulations 1(a,b,c,d) and computing the percentage difference on 31 March 1990 compared with 31 March 1987. WACCM3 (case 2) results, represented by the dashed line, was derived from the ensemble average of simulations 2(a,b,c,d) differenced with the ensemble average of simulations 2(w,x,y,z) for 31 March 1990.

SAGE II measurements and WACCM3 predictions show large enhancements in $NO_2$ on 31 March 1990 (Fig. 15, top): ~68% at 21 km for SAGE II; ~105% at 22 km for WACCM3 (case 1); and ~34% at 22 km for WACCM3 (case 2). These results point to a substantial downward transport of $NO_y$ (in general) and $NO_2$ (in particular) after the SPEs (also, see Fig. 14, top). Although there are differences between the model simulations and measurements in the absolute amount of enhanced $NO_2$ on 31 March 1990 as a result of the October 1989 SPEs, it is clear that these SPEs have led to an increase in $NO_2$. Some of the differences between WACCM3 and SAGE II $NO_2$ changes are probably related to interannual variability (see discussion in Jackman et al., 1995). Randall et al. (2006) also showed that varying meteorology plays a substantial role in determining the distribution of $NO_x$ in the NH middle atmosphere several months after energetic particle precipitation. Differences in medium-term changes in composition between the model and measurements are thus expected for these climatological WACCM3 runs.

The measured and modeled decreases in ozone are in qualitative agreement near 25 km (Fig. 15, bottom): ∼11% for SAGE II; ∼10% for WACCM3 (case 1); and ∼5% for WACCM3 (case 2). The measured and modeled ozone changes above 25 km indicate substantial variations with altitude. The polar regions have large interannual dynamical variations in both measurements and model simulations; thus, it is difficult to predict precisely the ozone impact over five months after this extremely large SPE period.

## 7 Conclusions

The WACCM3 has been used to study the short-term (days) and medium-term (months) constituent changes caused by SPEs over the 1963–2005 time period. The most pronounced atmospheric effects were caused by the very largest SPEs in this period and are concentrated in the polar regions. The four largest SPEs in the past 45 years (August 1972; October 1989; July 2000; and October–November 2003) have satellite instrument observations of atmospheric changes with which to compare. Generally, there is reasonable agreement between the WACCM3 predictions and the observations, especially for SPE-caused $NO_x$ enhancements and ozone depletion. There are, however, some disagreements between WACCM3 and satellite instrument observed enhancements of $HNO_3$, HOCl, ClO, $ClONO_2$, and $N_2O_5$, which tend to be higher in altitude than indicated in the measurements.

The atmospheric constituent effects can be summarized as follows: 1) Polar mesospheric $NO_x$ ($NO+NO_2$) increased by over 50 ppbv and mesospheric ozone decreased by over 30% during these very large SPE periods; 2) polar upper stratospheric and lower mesospheric $NO_x$ increased by over 10 ppbv, which was transported during polar night down to the middle stratosphere in a few weeks; 3) polar mid- to upper stratospheric ozone decreased over 20%; and 4) enhancements of $HNO_3$, HOCl, ClO, $ClONO_2$, and $N_2O_5$ were indirectly caused by the very large SPEs.

A manuscript in preparation will discuss the WACCM3 simulated long-term (months to years) atmospheric effects of very large SPEs.

*Acknowledgements.* This work was supported by the NASA Living With a Star Targeted Research and Technology Program and the NASA Atmospheric Composition Modeling and Analysis Program.

## References

Armstrong, T. P., Brundardt, C., and Meyer, J. E.: Satellite observations of interplanetary and polar cap solar particle fluxes from 1963 to the present, in: Weather and Climate Response to Solar Variations, edited by: McCormac, B. M., pp.71–79, Colorado Associated University Press, Boulder, 1983.

Banks, P. M.: Joule heating in the high-latitude mesosphere, J. Geophys. Res., 84, 6709–6712, 1979.

Brasseur, G. and Solomon, S.: Aeronomy of the Middle Atmosphere, D. Reidel Publising Company, Dordrecht, Holland, 245, 1984.

Crutzen, P. J., Isaksen, I. S. A., and Reid, G. C.: Solar proton events: Stratospheric sources of nitric oxide, Science, 189, 457–458, 1975.

Fabian, P., Pyle, J. A., and Wells, R. J.: The August 1972 solar proton event and the atmospheric ozone layer, Nature, 277, 458–460, 1979.

Forkman, P., Eriksson, P., Winnberg, A., Garcia, R. R., and Kinnison, D.: Longest continuous ground-based measurements of mesospheric CO, Geophys. Res. Lett., 30, 1532, doi:10.1029/2003GL016931, 2003.

Frederick, J. E.: Solar corpuscular emission and neutral chemistry in the Earth's middle atmosphere, J. Geophys. Res., 81, 3179–3186, 1976.

Garcia, R. R., Marsh, D., Kinnison, D., Boville, B., and Sassi, F.: Simulation of secular trends in the middle atmosphere, J. Geophys. Res., 112, D09301, doi:10.1029/2006JD007485, 2007.

Heath, D. F., Krueger, A. J., and Crutzen, P. J.: Solar proton event: influence on stratospheric ozone, Science, 197, 886–889, 1977.

Jackman, C. H. and McPeters, R. D.: The response of ozone to solar proton events during solar cycle 21: A theoretical interpretation, J. Geophys. Res., 90, 7955–7966, 1985.

Jackman, C. H. and McPeters, R. D.: Solar proton events as tests for the fidelity of middle atmosphere models, Physica Scripta, T18, 309—316, 1987.

Jackman, C. H. and McPeters, R. D.: "The Effect of Solar Proton Events on Ozone and Other Constituents," in: Solar Variability and its Effects on Climate, Geophys. Mon. 141, 305–319, 2004.

Jackman, C. H., Frederick, J. E., and Stolarski, R. S.: Production of odd nitrogen in the stratosphere and mesosphere: An intercomparison of source strengths, J. Geophys. Res., 85, 7495–7505, 1980.

Jackman, C. H., Douglass, A. R., Guthrie, P. D., and Stolarski, R. S.: The sensitivity of total ozone and ozone perturbation scenarios in a two-dimensional model due to dynamical inputs, J. Geophys. Res., 94, 9873–9887, 1989.

Jackman, C. H., Douglass, A. R., Rood, R. B., McPeters, R. D., and Meade, P. E.: Effect of solar proton events on the middle atmosphere during the past two solar cycles as computed using a two-dimensional model, J. Geophys. Res., 95, 7417–7428, 1990.

Jackman, C. H., Nielsen, J. E., Allen, D. J., Cerniglia, M. C., McPeters, R. D., Douglass, A. R., and Rood, R. B.: The effects of the October 1989 solar proton events on the stratosphere as computed using a three-dimensional model, Geophys. Res. Lett., 20, 459–462, 1993.

Jackman, C. H., Cerniglia, M. C., Nielsen, J. E., Allen, D. J., Zawodny, J. M., McPeters, R. D., Douglass, A. R., Rosenfield, J. E., and Rood, R. B.: Two-dimensional and three-dimensional model simulations, measurements, and interpretation of the influence of the October 1989 solar proton events on the middle atmosphere, J. Geophys. Res., 100, 11 641–11 660, 1995.

Jackman, C. H., Fleming, E. L., Chandra, S., Considine, D. B., and Rosenfield, J. E.: Past, present and future modeled ozone trends with comparisons to observed trends, J. Geophys. Res., 101, 28 753–28 767, 1996.

Jackman, C. H., Fleming, E. L., and Vitt, F. M.: Influence of extremely large solar proton events in a changing stratosphere, J. Geophys. Res., 105, 11 659–11 670, 2000.

Jackman, C. H., McPeters, R. D., Labow, G. J., Fleming, E. L., Praderass, C. J., and Russell, J. M.: Northern hemisphere atmospheric effects due to the July 2000 solar proton event, Geophys. Res. Lett., 28, 2883–2886, 2001.

Jackman, C. H., DeLand, M. T., Labow, G. J., Fleming, E. L., Weisenstein, D. K., Ko, M. K. W., Sinnhuber, M., and Russell, J. M.: Neutral atmospheric influences of the solar proton events in October–November 2003, J. Geophys. Res., 110, A09S27, doi:10.1029/2004JA010888, 2005a.

Jackman, C. H., DeLand, M. T., Labow, G. J., Fleming, E. L., Weisenstein, D. K., Ko, M. K. W., Sinnhuber, M., Anderson, J., and Russell, J. M.: The influence of the several very large solar proton events in Years 2000–2003 on the neutral middle atmosphere, Adv. Space Res., 35, 445–450, 2005b.

Jackman, C. H., Roble, R. G., and Fleming, E. L.: Mesospheric dynamical changes induced by the solar proton events in October–November 2003, Geophys. Res. Lett., 34, L04812, doi:10.1029/2006GL028328, 2007.

Krivolutsky, A., Ondraskova, A., and Lastovicka, J.: Photochemical response of neutral and ionized middle atmosphere composition to the strong solar proton event of October 1989, Adv. Sp. Res., 27, 1975–1981, 2001.

Krivolutsky, A., Kuminov, A., Vyushkova, T., Pereyaslova, N., and Nazarova, M.: Proton activity of the Sun during 23rd solar maximum and its response in ozonosphere of the Earth, Adv. Sp. Res., 31, 2151–2156, 2003.

Krivolutsky, A., Kuminov, A., and Vyushkova, T.: Ionization of the atmosphere caused by solar protons and its influence on ozonosphere of the Earth during 1994–2003, J. Atmos. Solar-Terr. Phys., 67, 105–117, 2005.

Krivolutsky, A. A., Klyuchnikova, A. V., Zakharov, G. R., Vyushkova, T. Y., and Kuminov, A. A.: Dynamical response of the middle atmosphere to solar proton event of July 2000: Three-dimensional model simulations, Adv. Sp. Res., 37, 1602–1613, 2006.

López-Puertas, M., Funke, B., Gil-López, S., von Clarmann, T., Stiller, G. P., Höpfner, M., Kellmann, S., Fischer, H., and Jackman, C. H.: Observation of $NO_x$ enhancement and ozone depletion in the Northern and Southern Hemispheres after the October–November 2003 solar proton events, J. Geophys. Res., 110, A09S43, doi:10.1029/2005JA011050, 2005a.

López-Puertas, M., Funke, B., Gil-López, S., Tsidu, G. M., Fischer, H., and Jackman, C. H.: $HNO_3$, $N_2O_5$, and $ClONO_2$ enhancements after the October–November 2003 solar proton events, J. Geophys. Res., 110, A09S44, doi:10.1029/2005JA011051, 2005b.

McPeters, R. D.: A nitric oxide increase observed following the July 1982 solar proton event, Geophys. Res. Lett., 13, 667–670, 1986.

McPeters, R. D. and Jackman, C. H.: The response of ozone to solar proton events during solar cycle 21: the observations, J. Geophys. Res., 90, 7945–7954, 1985.

McPeters, R. D., Jackman, C. H., and Stassinopoulos, E. G.: Observations of ozone depletion associated with solar proton events, J. Geophys. Res., 86, 12 071–12 081, 1981.

Nash, E. R., Newman, P. A., Rosenfield, J. E., and Schoeberl, M. R.: An objective determination of the polar vortex using Ertel's potential vorticity, J. Geophys. Res., 101, 9471–9478, 1996.

Natarajan, M., Remsberg, E. E., Deaver, L. E., and Russell III, J. M.: Anomalously high levels of $NO_x$ in the polar upper stratosphere during April, 2004: Photochemical consistency of HALOE observations, Geophys. Res. Lett., 31, L15113, doi:10.1029/2004GL020566, 2004.

Orsolini, Y. J., Manney, G. L., Santee, M. L., and Randall, C. E.: An upper stratospheric layer of enhanced $HNO_3$ following exceptional solar storms, Geophys. Res. Lett., 32, L12S01, doi:10.1029/2004GL021588, 2005.

Porter, H. S., Jackman, C. H., and Green, A. E. S.: Efficiencies for production of atomic nitrogen and oxygen by relativistic proton impact in air, J. Chem. Phys., 65, 154–167, 1976.

Randall, C. E., Siskind, D. E., and Bevilacqua, R. M.: Stratospheric $NO_x$ enhancements in the southern hemisphere polar vortex in winter and spring of 2000, Geophys. Res. Lett., 28, 2385–2388, 2001.

Randall, C. E., Harvey, V. L., Manney, G. L. , Orsolini, Y., Codrescu, M., Sioris, C., Brohede, S., Haley, C. S., Gordley, L. L., Zawodny, J. M., and Russell III, J. M.: Stratospheric effects of energetic particle precipitation in 2003–2004, Geophys. Res. Lett., 32, L05802, doi:10.1029/2004GL02203, 2005.

Randall, C. E., Harvey, V. L., Singleton, C. S., Bernath, P. F., Boone, C. D., and Kozyra, J. U.: Enhanced $NO_x$ in 2006 Linked to Strong Upper Stratospheric Arctic Vortex, Geophys. Res. Lett., 33, L18811, doi:10.1029/2006GL027160, 2006.

Randall, C. E., Harvey, V. L., Singleton, C. S., Bailey, S. M., Bernath, P. F., Codrescu, M., Nakajima, H., and Russell III, J. M.: Energetic particle precipitation effects on the southern hemisphere stratosphere in 1992–2005, J. Geophys. Res., 112, D08308, doi:10.1029/2006JD007696, 2007.

Reagan, J. B., Meyerott, R. E., Nightingale, R. W., Gunton, R. C., Johnson, R. G., Evans, J. E., Imhof, W. L., Heath, D. F., and Krueger, A. J.: Effects of the August 1972 solar particle events on stratospheric ozone, J. Geophys. Res., 86, 1473–1494, 1981.

Reid, G. C., Solomon, S., and Garcia, R. R.: Response of the middle atmosphere to the solar proton events of August-December 1989, Geophys. Res. Lett., 18, 1019–1022, 1991.

Richter, J. H. and Garcia, R. R.: On the forcing of the Mesospheric Semi-Annual Oscillation in the Whole Atmosphere Community Climate Model, Geophys. Res. Lett., 33, L01806, doi:10.1029/2005GL024378, 2006.

Rinsland, C. P., Boone, C., Nassar, R., Walker, K., Bernath, P., McConnell, J. C., and Chiou, L.: Atmospheric Chemistry Experiment (ACE) Arctic stratospheric measurements of $NO_x$ during February and March 2004: Impact of intense solar flares, Geophys. Res. Lett., 32, L16S05, doi:10.1029/2005GL022425, 2005.

Roble, R. G., Emery, B. A., Killeen, T. L., Reid, G. C., Solomon, S., Garcia, R. R., Evans, D. S., Carignan, G. R., Heelis, R. A., Hanson, W. B., Winningham, D. J., Spencer, N. W., and Brace, L. H.: Joule heating in the mesosphere and thermosphere during the 13 July 1982, solar proton event, J. Geophys. Res., 92, 6083–6090, 1987.

Rohen, G., von Savigny, C., Sinnhuber, M., Llewellyn, E. J., Kaiser, J. W., Jackman, C. H., Kallenrode, M.-B., Schroter, J., Eichmann, K.-U., Bovensmann, H., and Burrows, J. P.: Ozone depletion during the solar proton events of Oct./Nov. 2003 as seen by SCIAMACHY, J. Geophys. Res., 110, A09S39, doi:10.1029/2004JA010984, 2005.

Rusch, D. W., Gerard, J.-C., Solomon, S., Crutzen, P. J., and Reid, G. C.: The effect of particle precipitation events on the neutral and ion chemistry of the middle atmosphere, 1, Odd nitrogen, Planet. Space Sci., 29, 767–774, 1981.

Sassi, F., Garcia, R. R., Boville, B. A., and Liu, H.: On temperature inversions and the mesospheric surf zone, J. Geophys. Res., 107, 4380, doi:10.1029/2001JD001525, 2002.

Sassi, F., Kinnison, D., Boville, B. A., Garcia, R. R., and Roble, R.: Effect of El Nino-Southern Oscillation on the dynamical, thermal, and chemical structure of the middle atmosphere, J. Geophys. Res., 109, D17108, doi:10.1029/2003JD004434, 2004.

Semeniuk, K., McConnell, J. C., and Jackman, C. H.: Simulation of the October-November 2003 solar proton events in the CMAM GCM: Comparison with observations, Geophys. Res. Lett. 32, L15S02, doi:10.1029/2004GL022392, 2005.

Seppälä, A., Verronen, P. T., Kyrölä, E., Hassinen, S., Backman, L., Hauchecorne, A., Bertaux, J. L., and Fussen, D.: Solar proton events of October-November 2003: Ozone depletion in the Northern Hemisphere polar winter as seen by GOMOS/Envisat, Geophys. Res. Lett., 31, L19107, doi:10.1029/2004GL021042, 2004.

Seppälä, A., Verronen, P. T., Sofieva, V. F., Tamminen, J., Kyrölä, E., Rodger, C. J., and Clilverd, M. A.: Destruction of the tertiary ozone maximum during a solar proton event, Geophys. Res. Lett., 33, L07804, doi:10.1029/2005GL025571, 2006.

Solomon, S. and Crutzen, P. J.: Analysis of the August 1972 solar proton event including chlorine chemistry, J. Geophys. Res., 86, 1140–1146, 1981.

Solomon, S., Rusch, D. W., Gerard, J.-C., Reid, G. C., and Crutzen, P. J.: The effect of particle precipitation events on the neutral and ion chemistry of the middle atmosphere, 2, Odd hydrogen, Planet. Space Sci., 29, 885–892, 1981.

Solomon, S., Reid, G. C., Rusch, D. W., and Thomas, R. J.: Mesospheric ozone depletion during the solar proton event of 13 July 1982, 2, Comparison between theory and measurements, Geophys. Res. Lett., 10, 257–260, 1983.

Swider, W. and Keneshea, T. J.: Decrease of ozone and atomic oxygen in the lower mesosphere during a PCA event, Planet. Space Sci., 21, 1969–1973, 1973.

Swider, W., Keneshea T. J., and Foley, C. I.: An SPE disturbed D-region model, Planet. Space Sci., 26, 883–892, 1978.

Thomas, R. J., Barth, C. A., Rottman, G. J., Rusch, D. W., Mount, G. H., Lawrence, G. M., Sanders, R. W., Thomas, G. E., and Clemens, L. E.: Mesospheric ozone depletion during the solar proton event of 13 July 1982, 1, Measurements, Geophys. Res. Lett., 10, 257–260, 1983.

erronen, P. T., Turunen, E., Ulich, T., and Kyrola, E.: Modeling the effects of the October 1989 solar proton event on mesospheric odd nitrogen using a detailed ion and neutral chemistry model, Ann. Geophys., 20, 1967–1976, 2002, http://www.ann-geophys.net/20/1967/2002/.

Verronen, P. T., Seppala, A., Clilverd, M. A., Rodger, C. J., Kyrola, E., Enell, C.-F., Ulich, T., and Turunen, E.: Diurnal variation of ozone depletion during the October-November 2003 solar proton events, J. Geophys. Res., 110, A09S32, doi:10.1029/2004JA010932, 2005.

Verronen, P. T., Seppala, A., Kyrola, E., Tamminen, J., Pickett, H. M., and Turunen, E.: Production of odd hydrogen in the mesosphere during the January 2005 solar proton event, Geophys. Res. Lett., 33, L24811, doi:10.1029/2006GL028115, 2006.

von Clarmann, T., Glatthor, N., Hopfner, M., Kellmann, S., Ruhnke, R., Stiller, G. P., and Fischer, H.: Experimental evidence of perturbed odd hydrogen and chlorine chemistry after the October 2003 solar proton events, J. Geophys. Res., 110, A09S45, doi:10.1029/2005JA011053, 2005.

Vitt, F. M. and Jackman, C. H.: A comparison of sources of odd nitrogen production from 1974 through 1993 in the Earth's middle atmosphere as calculated using a two-dimensional model, J. Geophys. Res., 101, 6729–6739, 1996.

Vitt, F. M., Armstrong, T. P., Cravens, T. E., Dreschhoff, G. A. M., Jackman, C. H., and Laird, C. M.: Computed contributions to odd nitrogen concentrations in the Earth's polar middle atmosphere by energetic charged particles, J. Atmos. Solar-Terr. Phys., 62, 669–683, 2000.

Warneck, P., Cosmic radiation as a source of odd nitrogen in the stratosphere, J. Geophys. Res., 77, 6589–6591, 1972.

Weeks, L. H., CuiKay, R. S., and Corbin, J. R.: Ozone measurements in the mesosphere during the solar proton event of 2 November 1969, J. Atmos. Sci., 29, 1138–1142, 1972.

Zadorozhny, A. M., Tuchkov, G. A., Kikhtenko, V. N., Lastovicka, J., Boska, J., and Novak, A.: Nitric oxide and lower ionosphere quantities during solar particle events of October 1989 after rocket and ground-based measurements, J. Atmos. Terr. Phys., 54, 183–192, 1992.

**Table 1.** Largest 15 Solar Proton Event Periods in Past 45 Years.

| Date of SPE(s) | Rank | Computed $NO_y$ Production In Middle Atmosphere (Gigamoles[1]) |
|---|---|---|
| 19–27 October 1989 | 1 | 11. |
| 2–10 August 1972 | 2 | 6.0 |
| 14–16 July 2000 | 3 | 5.8 |
| 28–31 October 2003 | 4 | 5.6 |
| 5–7 November 2001 | 5 | 5.3 |
| 9–11 November 2000 | 6 | 3.8 |
| 24–30 September 2001 | 7 | 3.3 |
| 13–26 August 1989 | 8 | 3.0 |
| 23–25 November 2001 | 9 | 2.8 |
| 2–7 September 1966 | 10 | 2.0 |
| 15–23 January 2005 | 11 | 1.8 |
| 29 September–3 October 1989 | 12 | 1.7 |
| 28 January–1 February 1967 | 13 | 1.6 |
| 23-29 March 1991 | 14 | 1.5 |
| 7–17 September 2005 | 15 | 1.5 |

[1] Gigamole=$6.02\times10^{32}$ atoms and molecules

**Table 2.** Description of WACCM3 simulations.

| Simulation designation | Number of realizations | Time period | SPEs included |
|---|---|---|---|
| 1 (a, b, c, d) | 4 | 1963–2005 | Yes |
| 2 (a, b, c, d) | 4 | 1 January 1989–31 December 1991 | Yes |
| 2 (w, x, y, z) | 4 | 1 January 1989–31 December 1991 | No |
| 3 (a, b, c, d) | 4 | 2 July–30 September 2000 | Yes |
| 3 (w, x, y, z) | 4 | 2 July–30 September 2000 | No |
| 4 (a) | 1 | 25 October–14 November 2003 | Yes |
| 4 (w) | 1 | 25 October–14 November 2003 | No |

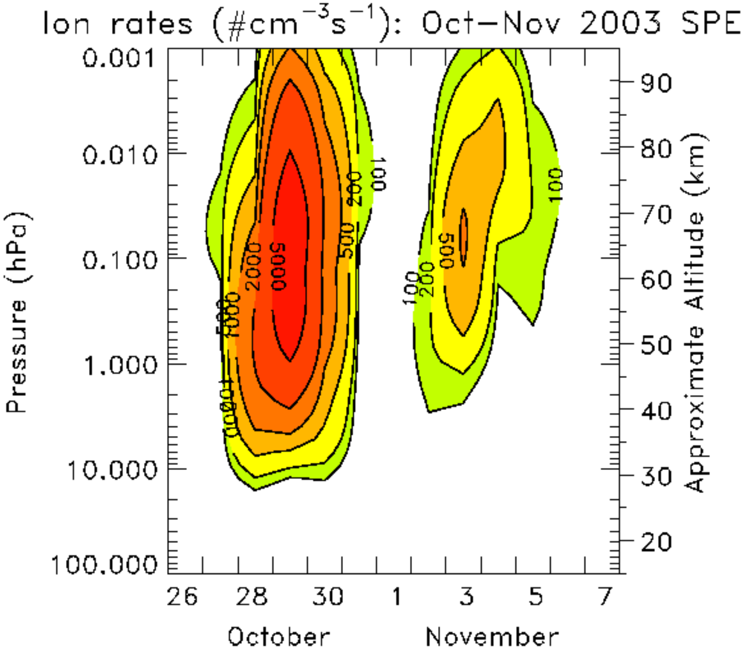

**Fig. 1.** Daily average ion pair production rates using the GOES 11 proton flux measurements for 26 October through 7 November 2003. Contour levels are 100, 200, 500, 1000, 2000, and 5000 cm$^{-3}$ s$^{-1}$.

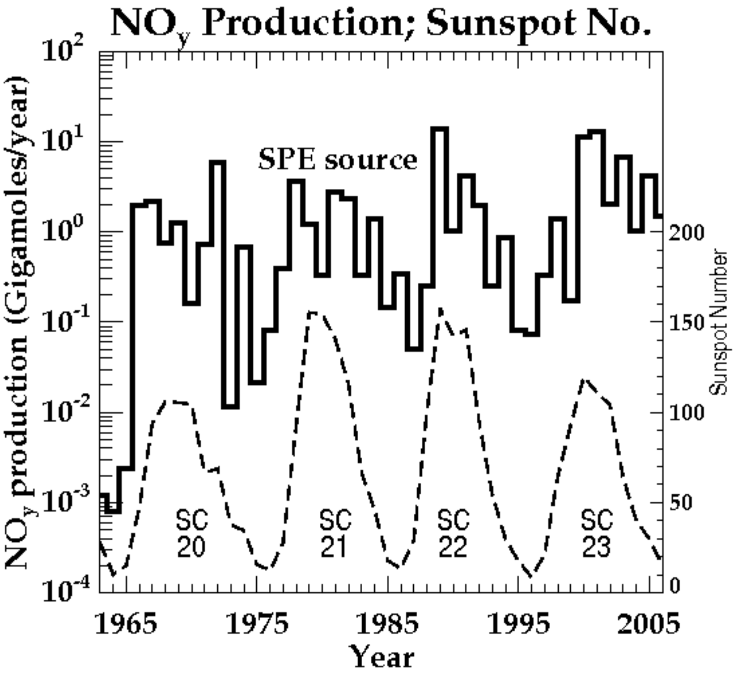

**Fig. 2.** The amount of NO$_y$ gigamoles produced per year in the middle atmosphere by SPEs is indicated by the histogram with the left ordinate showing the scale; the annual averaged sunspot numbers are indicated by the dashed line with the right ordinate showing the scale; and the number of the solar cycle (SC) is also indicated (SC 19, SC 20, SC 21, SC 22, SC 23). Plotted values for NO$_y$ production are taken from Jackman et al. (1980, 1990, 2005b), Vitt and Jackman (1996), and recent computations.

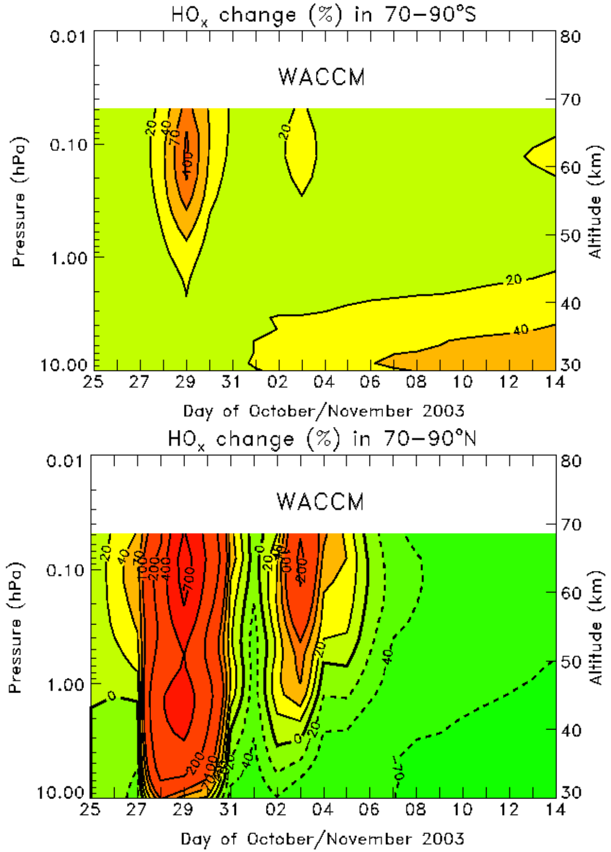

**Fig. 3.** Temporal evolution of HO$_x$ (H, OH, HO$_2$) abundance changes relative to 25 October during and after the October–November 2003 SPEs for the Southern Hemisphere (70–90° S) (left) and Northern Hemisphere (70–90° N) (right) polar caps predicted by WACCM simulation 4(a). Contour levels plotted are –70, –40, –20, 0, 20, 40, 70, 100, 200, 400, and 700%.

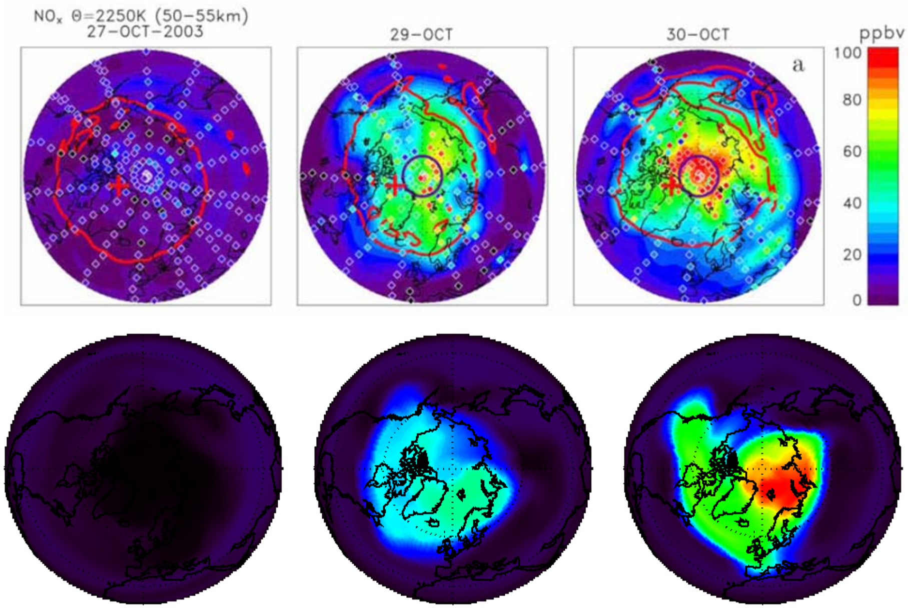

**Fig. 4.** Top three plots are taken from Fig. 2 of Lopez-Puertas et al. (2005) and show the Northern Hemisphere polar atmospheric abundance of NO$_x$ (ppbv) for days 27, 29, and 30 October 2003, which is just before and during a major solar proton event at a potential temperature of 2250 K. Contours are zonally smoothed within 700 km. Individual measurements are represented by diamonds. The polar vortex edge is represented with a red curve and the geomagnetic pole is marked with a red plus sign. The circle around the pole represents the polar night terminator. Bottom three plots are from WACCM3 simulation 4(a) for the same three days at 0.55 hPa (~55 km).

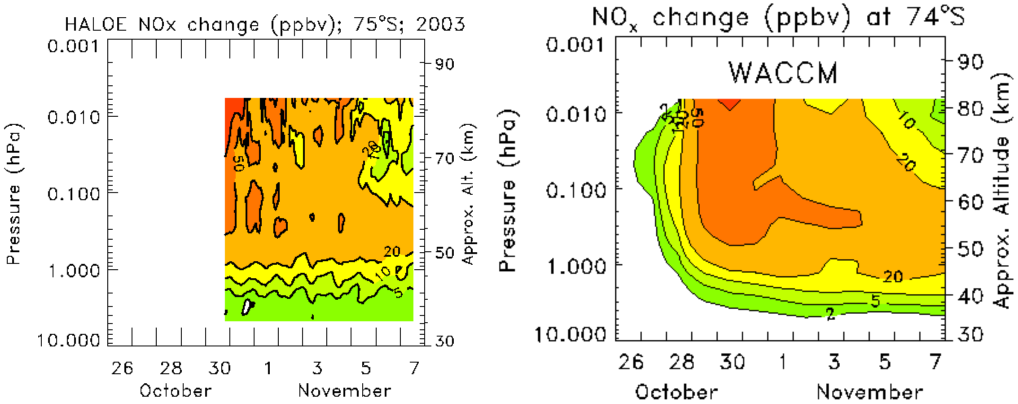

**Fig. 5.** Left plot is taken from Fig. 7 of Jackman et al. (2005a) and shows the polar Southern Hemisphere NO$_x$ change caused by the late October–early November 2003 SPEs beyond the ambient atmosphere amounts measured 12–15 October 2003. Right plot is derived from WACCM3 simulation 4(a) and indicates the NO$_x$ change caused by the October–November 2003 SPEs beyond the ambient atmosphere amounts on 25 October (before the SPEs). Contour levels plotted are 2, 5, 10, 20, 50, and 100 ppbv.

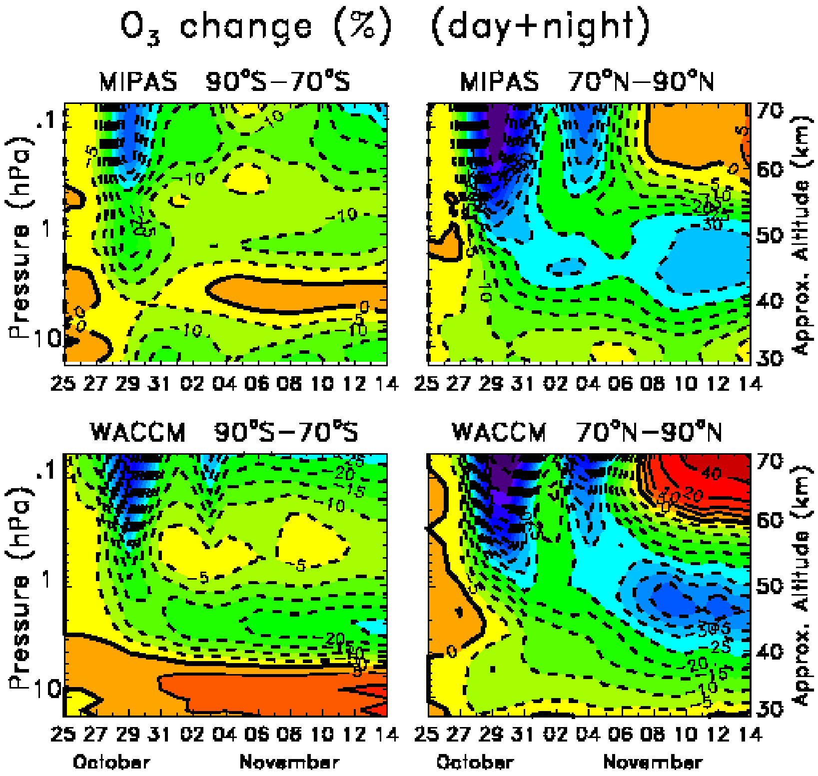

**Fig. 6.** Top two plots are taken from Fig. 4 of Lopez-Puertas et al. (2005) and show the temporal evolution of changes in ozone relative to 25 October during and after the October–November 2003 SPEs for the Southern Hemisphere (SH) (70–90° S) (left) and Northern Hemisphere (NH) (70–90° N) (right) polar caps. Bottom two plots are derived from WACCM3 simulation 4(a) and indicate ozone changes relative to 25 October. Contour levels plotted are –70, –65, –60, –55, –50, –45, –40, –35, –30, –25, –20, –15, –10, –5, 0, 5, 10, 20, and 40%.

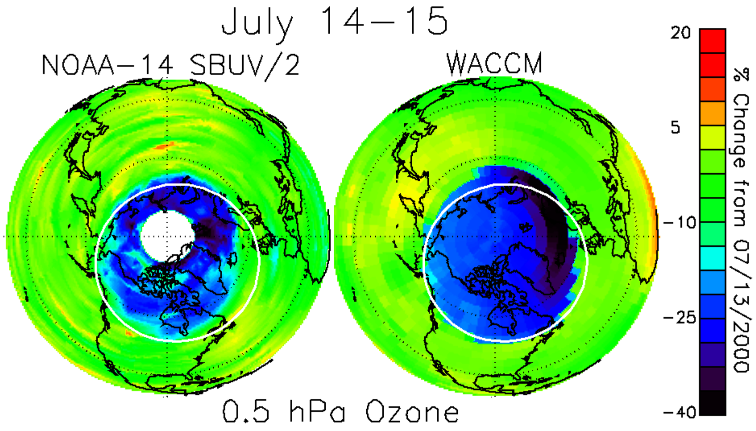

**Fig. 7.** Left plot shows NOAA-14 SBUV/2 Northern Hemisphere polar ozone percentage change at 0.5 hPa from 13 July 2000 (before the SPE) to 14–15 July 2000 (maximum proton intensity). Right plot shows WACCM3 "snapshot" using simulation 3(a) of polar ozone percentage change at 0.5 hPa for 00:00 GMT from 13 July to 15 July 2000.

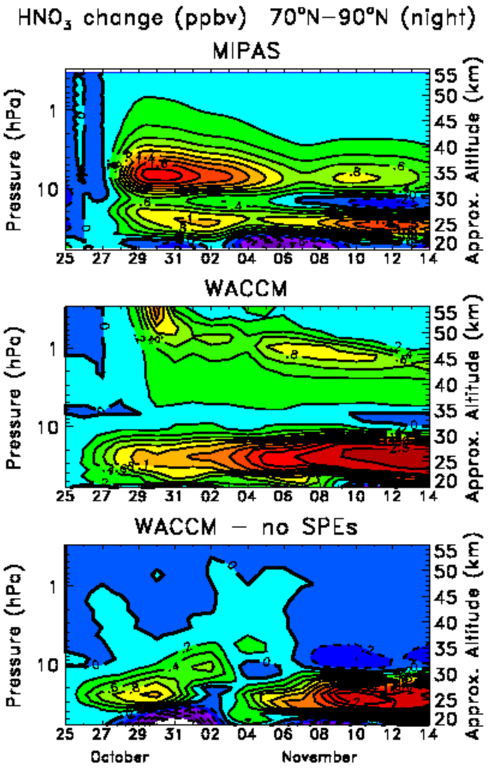

**Fig. 8.** Top plot is taken from Fig. 2a of Lopez-Puertas et al. (2005b) and shows the temporal evolution of MIPAS $HNO_3$ abundance changes relative to 26 October for nighttime in the polar Northern Hemisphere (70–90° N). Middle plot is derived from WACCM3 simulation 4(a), which includes SPEs, and indicates $HNO_3$ changes relative to 25 October for night in 70–90° N. Bottom plot is derived from WACCM3 simulation 4(w), which does not include SPEs, and indicates $HNO_3$ changes relative to 25 October for night in 70–90° N. Contour levels plotted are –0.6, –0.4, –0.2, 0.0, 0.2, 0.4, 0.6, 0.8, 1.0, 1.2, 1.4, 1.6, 1.8, 2.0, 2.5, and 3.0 ppbv.

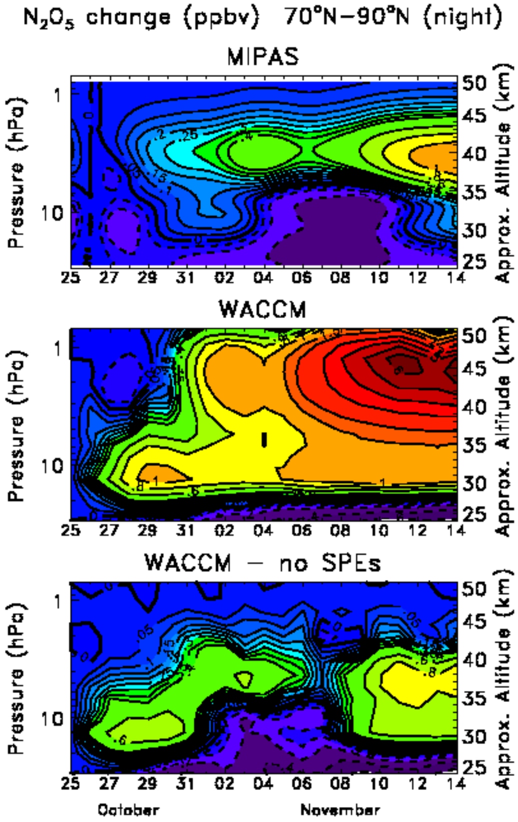

**Fig. 9.** Top plot is taken from Fig. 5 of Lopez-Puertas (2005b) and shows the temporal evolution of MIPAS $N_2O_5$ abundance changes relative to 26 October for nighttime in the polar Northern Hemisphere (70–90° N). Middle plot is derived from WACCM3 simulation 4(a) and indicates $N_2O_5$ changes relative to 25 October for night in 70–90° N. Bottom plot is derived from WACCM3 simulation 4(w) indicates $N_2O_5$ changes relative to 25 October for night in 70–90° N. Contour levels plotted are –0.6, –0.4, –0.2, –0.1, –0.05, 0.0, 0.05, 0.1, 0.15, 0.2, 0.25, 0.3, 0.35, 0.4, 0.6, 0.8, 1.0, 1.5, 2, 3, 4, 5, and 6 ppbv.

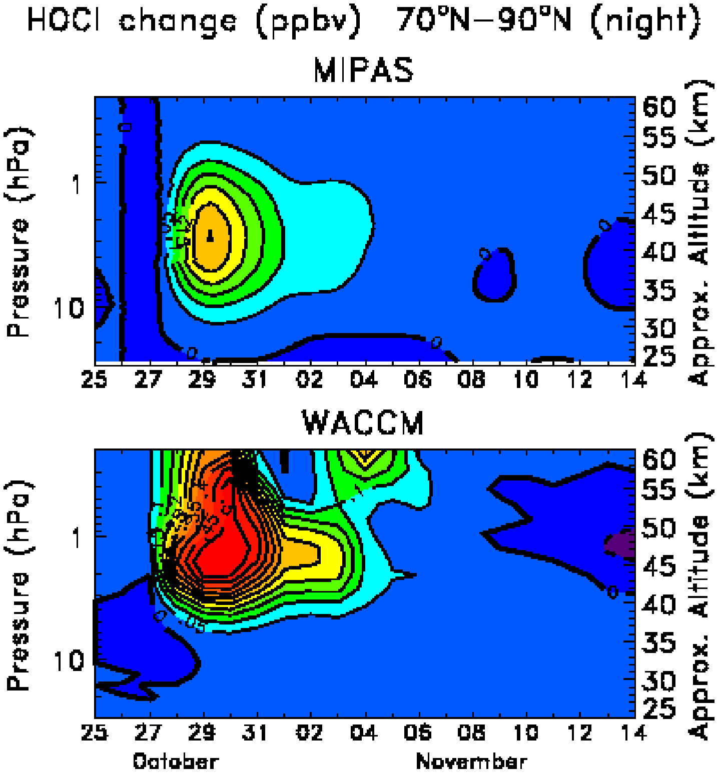

**Fig. 10.** Top plot is taken from Fig. 1 (middle) of von Clarmann et al. (2005) and shows the temporal evolution of MIPAS HOCl abundance changes relative to 26 October for nighttime in the polar Northern Hemisphere (70–90° N). Bottom plot is derived from WACCM3 simulation 4(a) and indicates HOCl changes relative to 25 October for night in 70–90° N. Contour levels for the bottom plot are –0.05, 0.0, 0.05, 0.1, 0.15, 0.2, 0.25, 0.3, 0.35, 0.4, 0.45, and 0.5 ppbv.

Title Page
Abstract | Introduction
Conclusions | References
Tables | Figures
◀◀ | ▶▶
◀ | ▶
Back | Close
Full Screen / Esc
Printer-friendly Version
Interactive Discussion

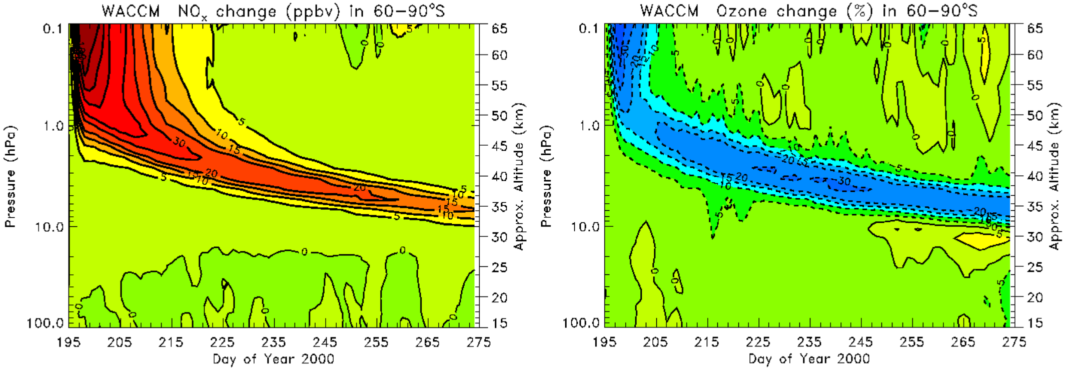

**Fig. 11.** Derived from WACCM3 output showing the difference of the ensemble average of simulations 3(a,b,c,d) compared to the ensemble average of simulations 3(w,x,y,z) for the latitude band 60–90° S from day 195 (13 July) through day 275 (1 October) for year 2000. Left plot indicates $NO_x$ change with contour levels of 0, 5, 10, 15, 20, 30, 40, 60, 80, and 100 ppbv. Right plot indicates ozone change with contour levels of –40, –30, –20, –15, –10, –5, 0, and 5%.

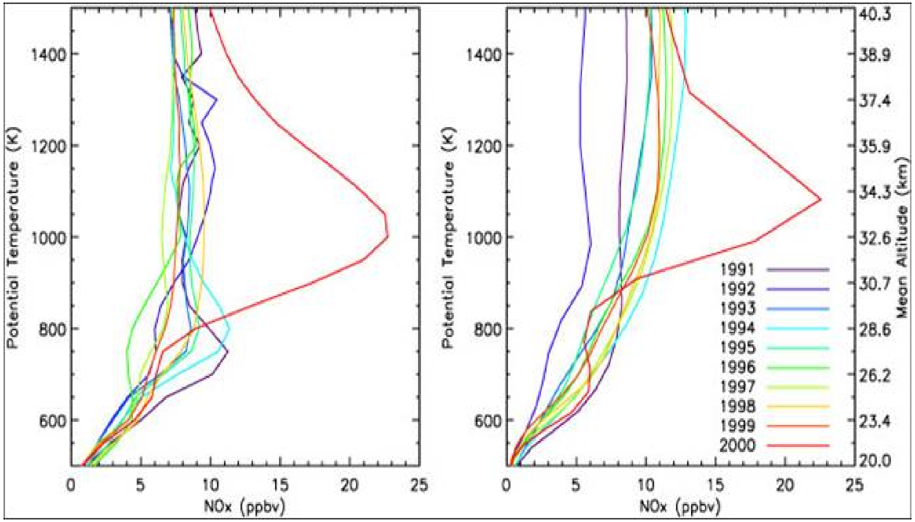

**Fig. 12.** Left plot is an adaptation of Fig. 5a of Randall et al. (2001) showing Southern Hemisphere (SH) polar vortex HALOE $NO_x$ (ppbv) profiles in September/October for years 1991–2000. Right plot shows WACCM3 simulation 1(a) predicted SH polar vortex $NO_x$ (ppbv) profiles for the same periods.

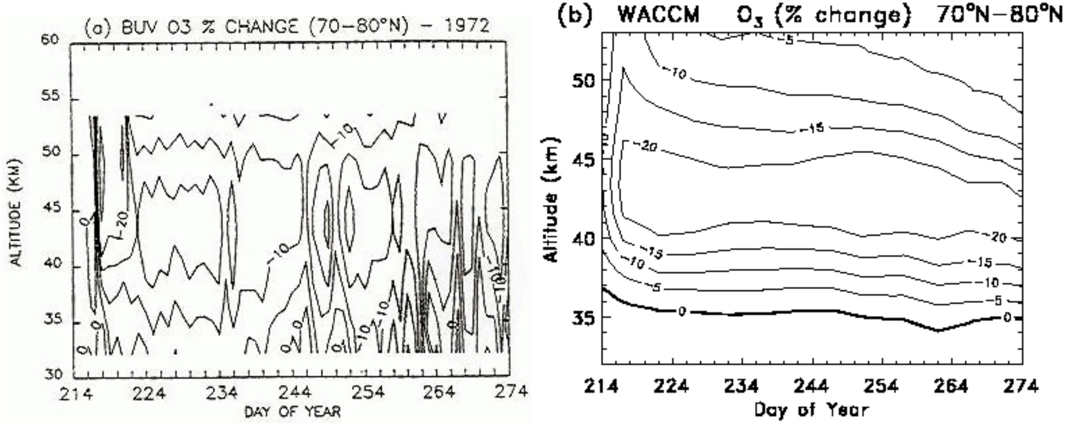

**Fig. 13.** Plot **(a)** is taken from Fig. 6 of Jackman et al. (1990) and shows the temporal evolution of measured ozone abundance changes in 1972 relative to 1970 by the backscattered ultraviolet (BUV) instrument aboard the Nimbus 4 satellite for the latitude band 70–80° N. Plot **(b)** is derived from the WACCM3 ensemble average of simulations 1(a,b,c,d) and indicates ozone changes in 1972 relative to 1970 in the same latitude bands. Contour levels plotted are –30, –20, –15, –10, –5, and 0%.

Title Page
Abstract
Introduction
Conclusions
References
Tables
Figures
◀
▶
Back
Close
Full Screen / Esc
Printer-friendly Version
Interactive Discussion
EGU

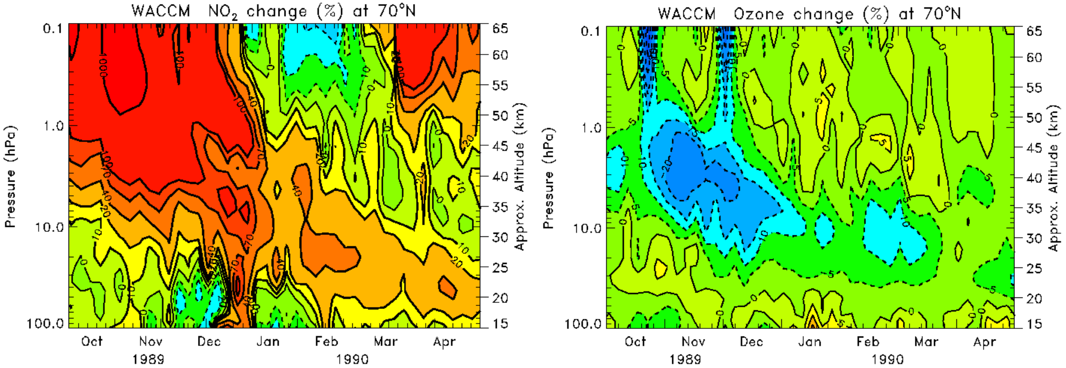

**Fig. 14.** Temporal evolution of WACCM3-computed percentage ozone change in 1989 for the ensemble average of simulations 2(a,b,c,d) average compared to the ensemble average of simulations 2(w,x,y,z) at 70° N for $NO_2$(top) and Ozone (bottom). Contour levels for $NO_2$ are –40, –20, –10, 0, 10, 20, 40, 70, 100, and 1000%. Contour levels for Ozone are –20, –15, –10, –5, 0, 5, 10, and 15%.

Title Page

Abstract | Introduction

Conclusions | References

Tables | Figures

◀▌ | ▶▌

◀ | ▶

Back | Close

Full Screen / Esc

Printer-friendly Version

Interactive Discussion

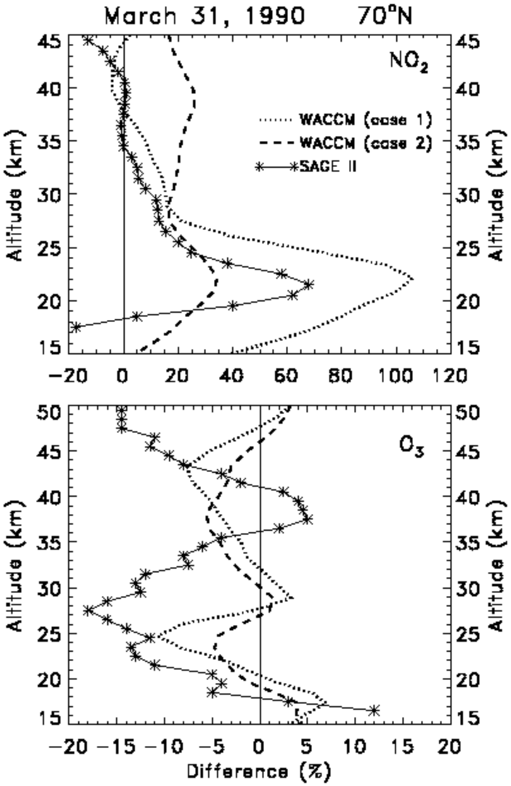

**Fig. 15.** SAGE II measurements (solid line) and WACCM3 predictions (dashed and dotted lines) for 70° N zonal mean percentage change for 31 March 1990 for constituents (top) $NO_2$ and (bottom) $O_3$. SAGE II results were derived by computing the percentage difference on 31 March 1990 compared with 31 March 1987. WACCM3 (case 1) was derived using the ensemble mean of simulations 1(a,b,c,d) and computing the percentage difference on 31 March 1990 compared with 31 March 1987. WACCM3 (case 2) was derived from the ensemble average of simulations 2(a,b,c,d) differenced with the ensemble average of simulations 2(w,x,y,z) for 31 March 1990.